A Journal of the Gesellschaft Deutscher Chemiker

Angewandte International Edition GDCh Chemie

www.angewandte.org

Accepted Article

Title: Room Temperature Activation of H_2 by a Surface Frustrated Lewis Pair

Authors: Lu Wang, Tingjiang Yan, Rui Song, Wei Sun, Yuchan Dong, Jiuli Guo, Zizhong Zhang, Xuxu Wang, and Geoffrey A. Ozin

To be cited as: *Angew. Chem. Int. Ed.* 10.1002/anie.201904568
Angew. Chem. 10.1002/ange.201904568

Link to VoR: http://dx.doi.org/10.1002/anie.201904568
http://dx.doi.org/10.1002/ange.201904568

WILEY-VCH

10.1002/anie.201904568

WILEY-VCH

Room Temperature Activation of H_2 by a Surface Frustrated Lewis Pair

Lu Wang[a], ‡, Tingjiang Yan[a], [b], ‡,*, Rui Song[a], [c], Wei Sun[a], Yuchan Dong[a], Jiuli Guo[a], [d], Zizhong Zhang[e], Xuxu Wang[e], Geoffrey A. Ozin[a],*

Abstract: Surface Frustrated Lewis Pairs (SFLPs) have been implicated in the gas-phase heterogeneous (photo)catalytic hydrogenation of CO_2 to CO and CH_3OH by $In_2O_{3-x}(OH)_y$. A key step in the reaction pathway is envisioned to be the heterolysis of H_2 on a proximal Lewis acid-Lewis base Pair, the SFLP, the chemistry of which is described as In•••In-OH + H_2 → In-OH_2^+•••In-H^-. The product of the heterolysis, thought to be a protonated hydroxide Lewis base In-OH_2^+ and a hydride coordinated Lewis acid In-H^-, can react with CO_2 to form either CO or CH_3OH. While the experimental and theoretical evidence is compelling for heterolysis of H_2 on the SFLP, all conclusions derive from indirect proof, and direct observation remains lacking. Unexpectedly, we have discovered rhombohedral $In_2O_{3-x}(OH)_y$ can enable dissociation of H_2 at room temperature, which allows its direct observation by several analytical techniques. The collected analytical results lean towards the heterolysis rather than the homolysis reaction pathway.

A frustrated Lewis pair (FLP) is a chemical system, consisting of both a Lewis acid and a Lewis base, sterically prevented from forming a Lewis acid-Lewis base adduct[1]. This behavior, well known in molecular organic compounds in solution, provides a platform for activating or dissociating small molecules; for instance, H_2 and CO_2[2]. Practical implementation of these homogeneous FLP systems requires recovery/purification/separation of product and catalysts. It is highly desirable therefore, to develop heterogeneous FLP analogues, in order to overcome the challenges confronted when working under homogeneous conditions[3].

[a] Dr. Lu Wang, Prof. Tingjiang Yan, Rui Song, Wei Sun, Yuchan Dong, Jiuli Guo, and Prof. Geoffrey A. Ozin
Department of Chemistry
University of Toronto
80 St. George Street, Toronto, Ontario M5S3H6 (Canada)
E-mail: ytj@qfnu.edu.cn
E-mail: gozin@chem.utoronto.ca
[b] Prof. Tingjiang Yan
College of Chemistry and Chemical Engineering
Qufu Normal University
Qufu, Shandong 273165 (P. R. China)
[c] Rui Song
International Research Center for Renewable Energy & State Key Laboratory of Multiphase Flow in Power Engineering
Xi'an Jiaotong University
Xi'an, Shanxi 710049 (P. R. China)
[d] Jiuli Guo
Department of Chemistry
Nankai University
Tianjin 300071 (P. R. China)
[b] Prof. Zizhong zhang and Prof. Xuxu Wang
State Key Laboratory of Photocatalysis on Energy and Environment, College of Chemistry
Fuzhou University
Fuzhou 350108 (P. R. China)
[‡] These authors contributed equally to this work.

Supporting information for this article is given via a link at the end of the document.

Dissociation of H_2 is ubiquitous in homogeneously and heterogeneously catalysed hydrogenation reactions, such as the CO_2 reduction reaction.[2a, 2d, 3f, 3g], [3l, 4] In the case of the surface frustrated Lewis pair (SFLP), the only evidence for the dissociation of H_2 stems from Density Functional Theory (DFT), and experimental evidence remains lacking.[3e, 4a, 5]

Recently we have discovered that the rhombohedral polymorph of rh-$In_2O_{3-x}(OH)_y$ is around two orders of magnitude more reactive than the cubic form of c-$In_2O_{3-x}(OH)_y$ for the production of CO or CH_3OH by the heterogeneous hydrogenation of gaseous CO_2.[6] In order to understand this significant difference in reactivity between these two polymorphs, we sought ways of dissecting the surface chemistry into the individual H_2 and CO_2 steps to gain an insight into the actual H_2 + CO_2 reaction pathway. To our surprise, we discovered that H_2 reacted at room temperature with rh-$In_2O_{3-x}(OH)_y$, a chemistry discovery which bodes well for a wide range of transition metal free hydrogenation reactions[2a, 7].

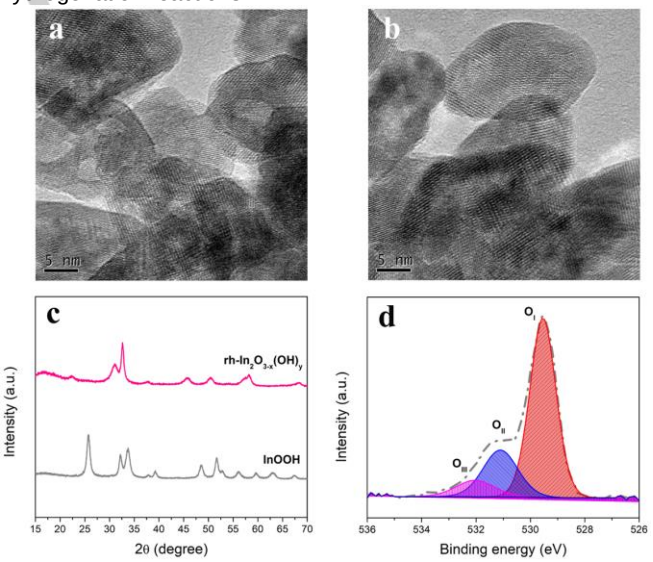

Figure 1. Characterization of as-synthesized rh-$In_2O_{3-x}(OH)_y$ nanocrystals. High-resolution transmission electron microscopy images of (a) InOOH and (b) rh-$In_2O_{3-x}(OH)_y$; (c) PXRD patterns of InOOH and rh-$In_2O_{3-x}(OH)_y$; (d) High resolution O 1s core level XPS of rh-$In_2O_{3-x}(OH)_y$. De-convolution of the O 1s XPS exhibits three distinct peaks at 529.54 eV (O_I), 531.11 eV (O_{II}) and 532.03 eV (O_{III}), which can be assigned as surface oxide, oxygen vacancies and hydroxyl groups, respectively.

The synthesis of rh-$In_2O_{3-x}(OH)_y$ nanocrystals employs temperature-controlled dehydroxylation of InOOH nanocrystals. Shown in **Figure 1a-b** are representative transmission electron microscopy (TEM) images of InOOH and rh-$In_2O_{3-x}(OH)_y$ nanocrystals with a similar particle size of ~20nm. The powder X-ray diffraction (PXRD) patterns of the precursors and prepared samples are shown in **Figure 1c**, which revealed the formation of a phase-pure, corundum structure-type, rhombohedral $In_2O_{3-x}(OH)_y$. X-ray photoelectron spectroscopy (XPS) provides

10.1002/anie.201904568

invaluable information on the elemental composition as well as oxidation state (**Figure S1**). The spin-orbit doublet In 3d core level XPS ionization potentials at 443.97 eV and 451.47 eV confirm the oxidation state of In(III) and the formation of indium oxide. The O 1s core level XPS spectra shown in **Figure 1d** can be fitted into 3 distinct peaks at 529.54 eV, 531.11 eV and 532.03 eV, which can be assigned to the ionization potential of oxide (O_I), oxygen vacancy (O_{II}) and hydroxide (O_{III}) groups, respectively. Gas-phase, flow catalysis studies define the most active form of rh-$In_2O_{3-x}(OH)_y$ for the production of CO or CH_3OH by hydrogenation of CO_2 to be the sample dehydroxylated at 350 °C.[6]

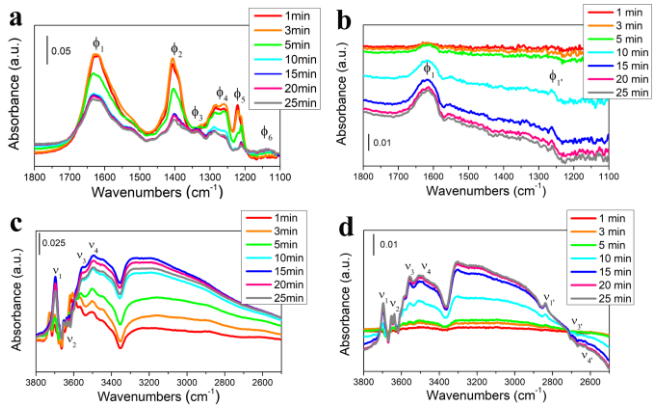

Figure 2. *Operando* DRIFT study of rh-$In_2O_{3-x}(OH)_y$ nanocrystals under different conditions. Surface species formed over rh-$In_2O_{3-x}(OH)_y$ in the hydride region under (a) H_2 atmosphere and (b) D_2 atmosphere; hydroxyl region under (c) H_2 atmosphere and (d) D_2 atmosphere. Conditions: room temperature, atmospheric pressure, 3 sccm H_2 or D_2 and 17 sccm He. The $\phi_{x'}$ and $\nu_{x'}$ represent the D_2 isotope shifted peaks of ϕ_x and ν_x, respectively.

The diffuse reflectance infrared Fourier transform spectroscopy (DRIFTS) observations, notably reveal the growth of intense vibrational modes in the fingerprint hydroxyl stretching and deformation region and hydride stretching region. The ZnSe window of the *operando* DRIFTS cell provides access to the infrared vibrational fingerprint range 1000-4000 cm^{-1}. All of these modes show the expected harmonic oscillator D_2 isotope shift, $\sqrt{(D/H)} = \sqrt{2}$, diagnostic of vibrational modes involving hydroxyl and hydride species (**Figure 2a-c**).

In **Figure 2a**, ϕ_1 with peaks located at 1631 and 1615 cm^{-1} are attributed to the terminal In-H^- which are possibly overlapping with the vibrational modes of In-OH^+ (formed via proton migration) and In-OH_2^+.Then ϕ_2 at 1400 cm^{-1} can be possibly be assigned to In-H^- on an In(III) site with different Lewis acidity. For ϕ_3 at 1335 cm^{-1} and ϕ_6 around 1150 cm^{-1} that showed up at the 3rd DRIFTS scan after 5 minute recording, can likely be associated to a bridging In-H^--In, which can reduce the population of active SFLP sites and result in the decrease of the peak intensity relating to terminal In-H^-, In-OH^+ and In-OH_2^+. Similarly, ϕ_2, ϕ_4 and ϕ_5 with peaks in between 1220 and 1300 cm^{-1} might relate to In-H^- or In-OH_2^+ on a SFLP site with different Lewis acidity and Lewis basicity.[8]

Support for these species identification stems from their disappearance at higher temperatures, and along with the shift of the relatively board peak of ϕ_1 at 1613 cm^{-1} to $\phi_{1'}$ at 1263 cm^{-1} (In-D^- and In-OD_2^+), and shift out of range of ϕ_2 to ϕ_6 under D_2, (**Figure 2b** and **Figure S2-3**). The presence of both ϕ_1 and $\phi_{1'}$ under D_2 condition can be explained by isotopic H/D exchange and proton migration. In the hydroxyl stretching and deformation region (**Figure 2c**), ν_1 at ~3700 cm^{-1} indicates surface terminal In-OH^+ and In-OH_2^+ species, and ν_2 at ~3646 cm^{-1} may be a bridging In-OH^+-In, while ν_3 at ~3550 cm^{-1} indicates a protonated In-OH_2^+ for an In-OH with different Lewis basicity. The ν_4 peak at ~3485-3500 cm^{-1} is likely a hydroxyl group in a different surface site.[8a, 9] Under an atmosphere of D_2, ν_1, ν_3 and ν_4 shift to $\nu_{1'}$, $\nu_{3'}$ and $\nu_{4'}$, respectively (**Figure 2d**).

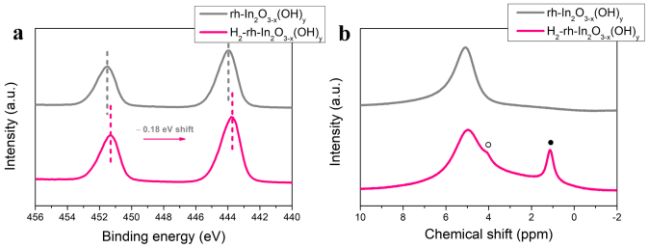

Figure 3. Characterization of room temperature H_2 heterolysis over rh-$In_2O_{3-x}(OH)_y$ nanocrystals. (a) High-resolution XPS of In 3d core levels. (b) *Ex situ* solid-state ^1H MAS-NMR spectra of rh-$In_2O_{3-x}(OH)_y$ nanocrystals, where ● (1.14 ppm) can be assigned as In-H^- and ○ (4.05 ppm) can be assigned as In-OH_2^+. Condition: before (grey) and after (pink) exposed to H_2 at atmospheric pressure and room temperature.

The corresponding high resolution XPS results, for rh-$In_2O_{3-x}(OH)_y$ exposed to H_2 at room temperature, shows a slight positive energy shift is observed for the hydroxide region of O 1s peak, while the In 3d peaks show slight negative energy shifts (**Figure 3a** and **Figure S4**). Furthermore, the In Auger LMM core level spectra were recorded and confirms the oxidation state of indium to be In(III) (**Figure S1c**). On exposure of rh-$In_2O_{3-x}(OH)_y$ to H_2 at room temperature, no visible change occurs to its yellowish colour, in accord with its optical spectrum, which shows no change in the UV absorption edge and remains non-absorbing in the Vis-NIR spectral range (**Figure S5**). Similarly, the solid state ^1H MAS NMR spectrum displays the growth of two new peaks: one with a chemical shift with respect to the adamantane reference at around 4.05 ppm, close to the peak at 5.1 ppm observed from pristine rh-$In_2O_{3-x}(OH)_y$, and the other with a chemical shift at 1.14 ppm (**Figure 3b**). During the process of heterolysis of H_2, In•••In-OH + H_2 → In-OH_2^+•••In-H^-, the Lewis base site In-OH becomes protonated, $InOH_2^+$ and induces a negative shift of In-OH from 5.1 ppm to the shoulder peak at 4.05 ppm, and the new peak at 1.14 ppm is associated with the formation of In-H^-.[10] Notably, the *in situ* electron paramagnetic resonance (EPR) spectrum of H_2 treated rh-$In_2O_{3-x}(OH)_y$ at both room temperature and 77 K displays no sign of paramagnetic species, and remains silent following H_2 treatment (**Figure S6**). The absence of a conduction electron signal around g=2.0 (3350 G) supports the heterolytic dissociation model of the H_2 molecule into charge-balancing H^+ and H^-.

10.1002/anie.201904568

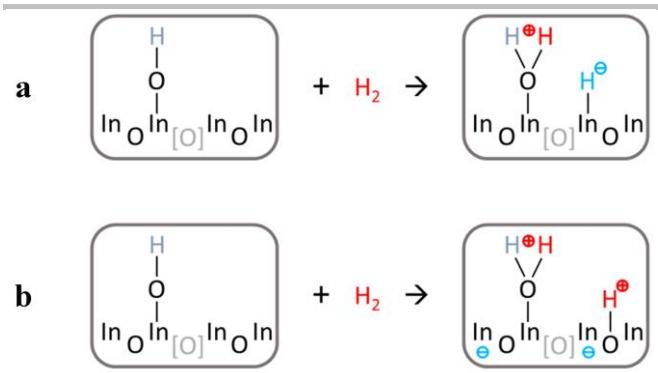

Figure 4. Illustration of the heterolysis and homolysis reaction pathways for the dissociation of H_2 on the SFLP in rh-$In_2O_{3-x}(OH)_y$. (a) H_2 heterolysis forms proton and hydride charge-balancing surface sites. (b) H_2 homolysis forms two protons and two charge-balancing electrons.

The surface of rh-$In_2O_{3-x}(OH)_y$ contains hydroxide groups and coordinately unsaturated indium sites, as illustrated in **Figure 4**. Chemically, these sites behave as a Lewis base and a Lewis acid, respectively, and together represent a SFLP, thought to play a key role in catalyzing the hydrogenation of CO_2 to CO and CH_3OH.[3l]

The first step in the catalytic cycle is purported to involve heterolysis of H_2 on the SFLP, as shown in **Figure 4a**, comprised of a proton bound to the hydroxide Lewis base site and a charge-balancing hydride attached to the coordinately unsaturated Lewis acid indium site. While the heterolysis scheme receives strong support from Density Functional Theory (DFT) simulations for both the ground and excited state reaction pathways, there currently exists no direct experimental evidence of its validity over a single component heterogeneous SFLP catalyst[3e, 4a, 5].

In this context, an alternative reaction pathway for H_2 activation that warrants consideration involves homolysis, as shown in **Figure 4b**. In this scheme, H_2 dissociates into two protons bound to hydroxide and/or oxide sites together with two charge-balancing electrons. The fate of these electrons could be multifold and include reduction of indium, trapping in oxygen vacancies and delocalized conduction bands.

The collected results obtained by the five analytical probes used in this study, shed new light on the reaction pathway that best describes the interaction of H_2 at room temperature with the SFLP in rh-$In_2O_{3-x}(OH)_y$.

To amplify, the DRIFTS results (**Figure 2a and 2c**) show the growth of new vibrational modes in the hydride region (ϕ_1 to ϕ_6) and hydroxyl region (v_1 to v_4), which all show the diagnostic D_2 isotope shift, $\sqrt{(D/H)} = \sqrt{2}$, expected for vibrational modes involving hydrogen motion in hydroxyl and hydride species (**Figure 2b and 2d**).

There is no doubt H_2 is being dissociated on the SFLP of rh-$In_2O_{3-x}(OH)_y$, however the ambiguity here is that the assigned indium hydride stretching mode, while in the expected frequency range, is difficult to unequivocally differentiate from an indium hydroxyl deformation mode, anticipated in the same range.

The high resolution XPS O 1s core level ionization potentials of rh-$In_2O_{3-x}(OH)_y$ can be resolved into three peaks assigned to oxide around 529.54 eV (O_I), oxygen vacancy at 531.11 eV (O_{II}) and hydroxyl at 532.03 eV (O_{III}) (**Figure 1d**). The line widths of these O 1s peaks are often broad and asymmetric because of multiple site occupancies of oxide, oxygen vacancies and hydroxyl in the surface and bulk regions of nanostructured rh-$In_2O_{3-x}(OH)_y$. The effective positive charge of the proton bonded to the oxide site of the hydroxyl causes the O 1s ionization potentials to shift to higher energy than the lattice oxide. In addition, the presence of an oxygen vacancy in the oxide coordination sphere of indium enhances binding of the remaining oxides to the indium, which is manifested as a shift to higher energy of the O 1s ionization potentials but lower than the O 1s of hydroxyl (**Figure S4**). The corresponding high resolution In 3d XPS results for nanostructured $In_2O_{3-x}(OH)_y$ exposed to H_2 at room temperature is shown in **Figure 3a**. The In $3d_{3/2,5/2}$ spin-orbit components are found to have ionization potentials around 443.97 eV. The C 1s energy range of rh-$In_2O_{3-x}(OH)_y$ shows a small amount of adventitious surface carbon around 284.5 eV, which is used as an energy calibration references (**Figure S1c**). Analogous to the O 1s line widths, these In 3d line widths are similarly broad and asymmetric because of multiple site occupancies in the surface and bulk of rh-$In_2O_{3-x}(OH)_y$.

On exposure of rh-$In_2O_{3-x}(OH)_y$ to H_2 at room temperature, a dramatic increase in the intensity and slight shift to high energy for the O 1s ionization potentials of the hydroxyl (**Figure S4**). This observation flags the dissociation of H_2 on the surface of rh-$In_2O_{3-x}(OH)_y$ with concomitant protonation and generation of additional hydroxides. Concurrently, the In $3d_{3/2,5/2}$ peaks undergo a notable shift to lower energy, implying the indium is experiencing a lower effective nuclear charge (**Figure 3a**). This behavior could arise from a coordinately unsaturated Lewis acidic surface indium site bonded to a highly nucleophilic hydride formed by heterolysis of H_2 on the SFLP site, which charge balances yet must dominate over the opposing effect of hydroxide or oxide protonation (**Figure 4**). Alternatively, homolysis of H_2 on hydroxide or oxide surface sites protonates these sites. The associated injection of charge balancing electrons into indium, oxygen vacancy or conduction band states could cause the In $3d_{3/2,5/2}$ peaks to shift to lower energy, providing it overrides the countering effect of oxide or hydroxyl protonation (**Figure 4**).

The two new chemical shifts observed in the ^{1}H MAS NMR provide some clarification of this hydroxyl-hydride ambiguity in the DRIFTS results (**Figure 3b**). The chemical shift around 4.05 ppm, which is close to the peak at 5.1 ppm observed for pristine rh-$In_2O_{3-x}(OH)_y$, signals a protonation of the oxygen of an In-OH or In-O-In site that can be associated with the dissociation of H_2 on the SFLP of rh-$In_2O_{3-x}(OH)_y$. The other chemical shift observed at 1.14 ppm is in the range anticipated for In-H$^-$. Based on Lenz's law, hydride is electron rich and is more shielded than reference adamantane, therefore typically hydrides occur at high field, which is low frequency. When hydride is bonded to a more electronegative element like indium (electronegativity: In>Ca), the hydride in In-H$^-$ should be less shielded than Ca-H$^-$ (~5 ppm) and therefore occur at a lower positive chemical shift than Ca-H$^-$, as we observe. To further support this proposal, another more electronegative metal, Ag was reported able to dissociate H_2 in an Ag-zeolite system and provide a new Ag-H peak at -0.1 ppm, which is more negative than the one we observed.[11] On the other hand, the proton in In-OH_2^+ appears shielded relative to In-OH as seen by the up-field chemical shift, could be evidence for proximal/adjacent Lewis base-Lewis acid in the SFLP In-OH_2^+…In-H$^-$ where the hydride near to the protons make them seem more electron rich than when they are well apart/isolated, and hence appear up-field rather than downfield. Assuming the ^{1}H MAS NMR proton and hydride assignments are correct, one

can deduce that the heterolytic H_2 dissociation pathway on the SFLP of rh-$In_2O_{3-x}(OH)_y$ is most favored.

The absence of any changes to the optical absorption edge and lack of any absorption in the visible to near infrared spectral range of rh-$In_2O_{3-x}(OH)_y$, following exposure to H_2 at room temperature, implies that its electronic band structure is hardly perturbed (**Figure S5**).[12] This observation supports the heterolysis model with maintenance of proton-hydride charge-balance and diamagnetism. Evidence for the latter deduction stems from the lack of any EPR signals diagnostic of unpaired electrons localized on the indium sites, trapped in oxygen vacancies or delocalized in conduction band states (**Figure S6**).

A few points worth mentioning that provide additional support for the heterolysis model, described in detail in a forthcoming paper, include the notable air stability of the H_2 treated rh-$In_2O_{3-x}(OH)_y$, the formation of both bicarbonate and formate with CO_2, production of formyl with CO, and reaction with C_2H_4 to form a surface ethyl functional group.

In conclusion, the accrued results of a suite of five insightful spectroscopy probes, DRIFTS, XPS, ^{1}H MAS NMR, EPR and UV-Vis-NIR, have provided a new window into how gaseous H_2 interacts with nanostructured rh-$In_2O_{3-x}(OH)_y$ at room temperature. Conclusions drawn from the integrated information derived from these analytical techniques lean towards the heterolysis over the homolysis reaction pathway. Inelastic neutron scattering and extended X-ray absorption fine structure studies, taken in conjunction with H-D kinetic isotope measurements, could provide additional structure and reactivity detail about the surface chemistry of the FLP in rh-$In_2O_{3-x}(OH)_y$.

Acknowledgements

GAO acknowledges the financial support of the Ontario Ministry of Research and Innovation (MRI), the Ministry of Economic Development, Employment and Infrastructure (MEDI), the Ministry of the Environment and Climate Change's (MOECC) and the Best in Science (BIS) Award. Acknowledged is additional support from the Ontario Center of Excellence (OCE) Solutions 2030 Challenge Fund, the Low Carbon Innovation Fund (LCIF), Imperial Oil, the University of Toronto Connaught Innovation Fund (CIF), the Connaught Global Challenge (CGC) Fund, and the Natural Sciences and Engineering Research Council of Canada (NSERC). T.Y. is thankful for financial support from the National Natural Science Foundation of China (21872081), Natural Science Foundation of Shandong Province (ZR2016BM04), and the Open Project Program of the State Key Laboratory of Photocatalysis on Energy and Environment (Grant No. SKLPEE-KF201711).

Keywords: Surface frustrated Lewis pair • Heterolytic H_2 dissociation • Room temperature • Indium oxide

[1] D. W. Stephan, *Science* **2016**, *354*, aaf7229.

[2] a) G. C. Welch, R. R. S. Juan, J. D. Masuda, D. W. Stephan, *Science* **2006**, *314*, 1124-1126; b) K. Chernichenko, A. Madarasz, I. Papai, M. Nieger, M. Leskela, T. Repo, *Nat Chem* **2013**, *5*, 718-723; c) M. A. Courtemanche, M. A. Legare, L. Maron, F. G. Fontaine, *J Am Chem Soc* **2014**, *136*, 10708-10717; d) K. Chernichenko, B. Kotai, I. Papai, V. Zhivonitko, M. Nieger, M. Leskela, T. Repo, *Angew Chem Int Edit* **2015**, *54*, 1749-1753; e) M. M. Hansmann, R. L. Melen, M. Rudolph, F. Rominger, H. Wadepohl, D. W. Stephan, A. S. K. Hashmi, *J Am Chem Soc* **2015**, *137*, 15469-15477; f) M. A. Legare, M. A. Courtemanche, E. Rochette, F. G. Fontaine, *Science* **2015**, *349*, 513-516; g) D. W. Stephan, *J Am Chem Soc* **2015**, *137*, 10018-10032; h) D. W. Stephan, G. Erker, *Angew Chem Int Edit* **2015**, *54*, 6400-6441.

[3] a) G. Lu, P. Zhang, D. Q. Sun, L. Wang, K. B. Zhou, Z. X. Wang, G. C. Guo, *Chem Sci* **2014**, *5*, 1082-1090; b) A. Primo, F. Neatu, M. Florea, V. Parvulescu, H. Garcia, *Nat Commun* **2014**, *5*, 5291; c) J. Y. Ye, J. K. Johnson, *Acs Catal* **2015**, *5*, 2921-2928; d) J. Y. Ye, J. K. Johnson, *Acs Catal* **2015**, *5*, 6219-6229; e) K. K. Ghuman, L. B. Hoch, P. Szymanski, J. Y. Y. Loh, N. P. Kherani, M. A. E-Sayed, G. A. Ozin, C. V. Singh, *J Am Chem Soc* **2016**, *138*, 1206-1214; f) X. Y. Sun, B. Li, T. F. Liu, J. Song, D. S. Su, *Phys Chem Chem Phys* **2016**, *18*, 11120-11124; g) J. Y. Xing, J. C. Buffet, N. H. Rees, P. Norby, D. O'Hare, *Chem Commun* **2016**, *52*, 10478-10481; h) J. Y. Ye, J. K. Johnson, *Catal Sci Technol* **2016**, *6*, 8392-8405; i) J. Jia, C. X. Qian, Y. C. Dong, Y. F. Li, H. Wang, M. Ghoussoub, K. T. Butler, A. Walsh, G. A. Ozin, *Chem Soc Rev* **2017**, *46*, 4631-4644; j) S. Zhang, Z. Q. Huang, Y. Y. Ma, W. Gao, J. Li, F. X. Cao, L. Li, C. R. Chang, Y. Qu, *Nat Commun* **2017**, *8,* 15266; k) Y. C. Dong, K. K. Ghuman, R. Popescu, P. N. Duchesne, W. J. Zhou, J. Y. Y. Loh, A. A. Jelle, J. Jia, D. Wang, X. K. Mu, C. Kubel, L. Wang, L. He, M. Ghoussoub, Q. Wang, T. E. Wood, L. M. Reyes, P. Zhang, N. P. Kherani, C. V. Singh, G. A. Ozin, *Adv Sci* **2018**, *5,* 1700732; l) L. Wang, M. Ghoussoub, H. Wang, Y. Shao, W. Sun, A. A. Tountas, T. E. Wood, H. Li, J. Y. Y. Loh, Y. C. Dong, M. K. Xia, Y. Li, S. H. Wang, J. Jia, C. Y. Qiu, C. X. Qian, N. P. Kherani, L. He, X. H. Zhang, G. A. Ozin, *Joule* **2018**, *2*, 1382-1382; m) L. Wang, G. Kehr, C. G. Daniliuc, M. Brinkkotter, T. Wiegand, A. L. Wubker, H. Eckert, L. Liu, J. G. Brandenburg, S. Grimme, G. Erker, *Chem Sci* **2018**, *9*, 4859-4865; n) L. He, T. E. Wood, B. Wu, Y. C. Dong, L. B. Hoch, L. M. Reyes, D. Wang, C. Kubel, C. X. Qian, J. Jia, K. Liao, P. G. O'Brien, A. Sandhel, J. Y. Y. Loh, P. Szymanski, N. P. Kherani, T. C. Sum, C. A. Mims, G. A. Ozin, *Acs Nano* **2016**, *10*, 5578-5586.

[4] a) K. K. Ghuman, T. E. Wood, L. B. Hoch, C. A. Mims, G. A. Ozin, C. V. Singh, *Phys Chem Chem Phys* **2015**, *17*, 14623-14635; b) Y. F. Zhao, Z. H. Li, M. Z. Li, J. J. Liu, X. W. Liu, G. I. N. Waterhouse, Y. S. Wang, J. Q. Zhao, W. Gao, Z. S. Zhang, R. Long, Q. H. Zhang, L. Gu, X. Liu, X. D. Wen, D. Ma, L. Z. Wu, C. H. Tung, T. R. Zhang, *Adv Mater* **2018**, *30,* 1803127; c) J. Ren, S. X. Ouyang, H. Xu, X. G. Meng, T. Wang, D. F. Wang, J. H. Ye, *Adv Energy Mater* **2017**, *7,* 1601657.

[5] M. Ghoussoub, S. Yadav, K. K. Ghuman, G. A. Ozin, C. V. Singh, *Acs Catal* **2016**, *6*, 7109-7117.

[6] T. Yan, L. Wang, Y. Liang, M. Makaremi, T. Wood, Y. Dai, B. Huang, A. A. Jelle, Y. Dong, G. A. Ozin, *Submitted* **2018**.

[7] M. Trunk, J. F. Teichert, A. Thomas, *J Am Chem Soc* **2017**, *139*, 3615-3618.

[8] a) H. Lee, Y. N. Choi, D. W. Lim, M. M. Rahman, Y. I. Kim, I. H. Cho, H. W. Kang, J. H. Seo, C. Jeon, K. B. Yoon, *Angew Chem Int Edit* **2015**, *54*, 13080-13084; b) X. F. Wang, L. Andrews, *J Phys Chem A* **2004**, *108*, 4440-4448; c) L. Andrews, X. F. Wang, *Angew Chem Int Edit* **2004**, *43*, 1706-1709; d) K. Raghavachari, Q. Fu, G. Chen, L. Li, C. H. Li, D. C. Law, R. F. Hicks, *J Am Chem Soc* **2002**, *124*, 15119-15124.

[9] a) J. Datka, B. Sulikowski, B. Gil, *J Phys Chem-Us* **1996**, *100*, 11242-11245; b) B. Gil, E. Broclawik, J. Datka, J. Klinowski, *J Phys Chem-Us* **1994**, *98*, 930-933.

[10] K. Hayashi, P. V. Sushko, Y. Hashimoto, A. L. Shluger, H. Hosono, *Nat Commun* **2014**, *5*, 3515.

[11] a) R. T. Sanderson, *J Am Chem Soc* **1983**, *105*, 2259-2261; b) T. Baba, N. Komatsu, H. Sawada, Y. Yamaguchi, T. Takahashi, H. Sugisawa, Y. Ono, *Langmuir* **1999**, *15*, 7894-7896; c) A. A. Gabrienko, S. S. Arzumanov, I. B. Moroz, A. V. Toktarev, W. Wang, A. G. Stepanov, *J. Phys. Chem. C* **2013**, *117*, 7690-7702.

[12] S. D. Lounis, E. L. Runnerstrom, A. Llordes, D. J. Milliron, *J. Phys. Chem. Lett.* **2014**, *5*, 1564-1574.

10.1002/anie.201904568

WILEY-VCH

Entry for the Table of Contents

COMMUNICATION

Room temperature heterolysis of H_2 on the surface fraustrated Lewis pair over rhombohedral $In_2O_{3-x}(OH)_y$.

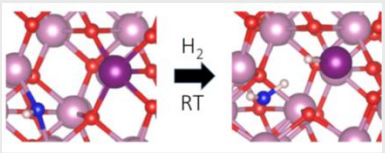

Lu Wang, Tingjiang Yan, Rui Song, Wei Sun, Yuchan Dong, Jiuli Guo, Zizhong Zhang, Xuxu Wang, Geoffrey A. Ozin**

Page No. – Page No.

Room Temperature Activation of H_2 by a Surface Frustrated Lewis Pair